Numerical Solution of the Incompressible Navier-Stokes Equations in Doubly-Connected Regions

DES R. SOOD*
Western Electric Company, Inc., Princeton, N.J.

AND

HAROLD G. ELROD JR.†
Columbia University, New York, N.Y.

A transient computational procedure for the numerical solution of the incompressible Navier-Stokes equations in doubly-connected domains is described. The tangential velocity boundary conditions are satisfied by introducing shear layers at the boundaries at each time-step. The requirement that the pressure be single-valued is explicitly included in the formulation. The computational procedure is applied to the viscous flow in the annulus between two eccentric cylinders when either of them is rotating. Transient and steady-state results are obtained for both Stokes flow (inertia neglected) and Navier-Stokes flow. Rotational speeds of the outer cylinder are explored for the entire extent of laminar flow and of the inner cylinder up to the point of incidence of Taylor vortices. The agreement between the steady-state numerical results and the exact analytical results for the Stokes flow is very good. It is believed that inclusion of inertia does not appreciably affect the solution accuracy.

I. Introduction

THE purpose of this paper is to describe a computational procedure for the numerical solution of two-dimensional, incompressible, viscous flow problems. The stream function, ψ, and the vorticity function, ω, are chosen as the primary dependent variables. In the past a number of authors, such as Fromm,[1] Thoman and Szewczyk,[4] and Runchal, Spalding, and Wolfshtein,[3] have proposed, ψ–ω, procedures for solution of the Navier-Stokes equations. However, these methods exhibit some lack of precision insofar as computation of the vorticity at the boundaries is concerned. Such inaccuracies at the boundary adversely affect the efficiency and accuracy of the solution procedures, because the transient flow development is determined by transport of the vorticity generated at the surfaces. Another deficiency in published procedures arises from a failure to account for the multiconnectedness of domains which include obstacles. To ensure single-valuedness of the pressure in a doubly-connected region, an explicit requirement must be made that the line integral of the normal derivative of the vorticity taken around the obstacle periphery vanish. To the best of our knowledge, previous authors have not done so.

In the current investigation, a new ψ–ω, computational procedure applicable to the solution of the two-dimensional, time-dependent, viscous, incompressible flow equations in a doubly-connected region is presented. The domain of interest is spanned by an orthogonal mesh. The differential equations are replaced by their finite-difference analogs and the resulting set of algebraic equations is solved iteratively. The tangential velocity boundary conditions are satisfied by introducing for each time-step shear layers of specified strength at the two boundaries. The vorticity thus generated at the surfaces diffuses into the flow-field. It is believed that this procedure simulates the physical phenomenon more realistically. The normal velocity boundary conditions at impervious boundaries, are satisfied by prescribing ψ to be zero at one of the boundaries, and time-dependent values at the others. The requirement of single-valuedness of the pressure for multiconnected regions yields constraints which are sufficient to determine these values uniquely. If the boundaries are permeable, the values of ψ can be adjusted to take care of the inflow and outflow. The vorticity at the surface is computed from a highly accurate finite-difference analog of the Poisson's equation relating stream function and vorticity.

II. Formulation and Algorithms

Consider a doubly-connected region, spanned by an orthogonal mesh of α, β-lines, as shown in Fig. 1. For ease in imposition of the boundary conditions, the coordinate system (α, β) is chosen so that the boundaries can be identified by the coordinate lines. The velocity boundary conditions are prescribed at $\alpha = \alpha_1$ and α_2. A numerical solution is sought to the Navier-Stokes equations in the region bounded by α_1 and α_2.

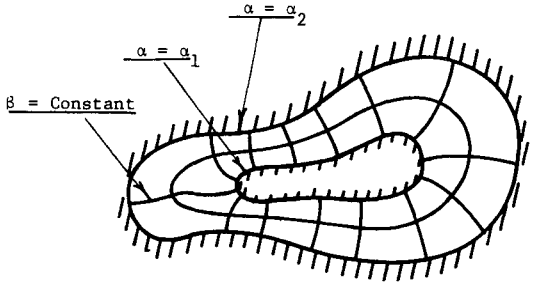

Fig. 1 Coordinate system.

Presented as Paper 72-113 at the AIAA 10th Aerospace Sciences Meeting, San Diego, Calif., January 17–19, 1972; submitted June 25, 1973; revision received November 29, 1973. This work was performed under Contract Nonr-4259 (14), Task NR 062, 360, supported by the Information Systems and Fluid Dynamics Branches of the Office of Naval Research, and was monitored by S. W. Doroff. The work reported here is part of a dissertation submitted by the first author, in partial fulfillment of the requirements of degree of Doctor of Engineering Science, to the School of Engineering and Applied Science of Columbia University, New York.

Index category: Nozzle and Channel Flow.

* Member of Research Staff. Associate Member AIAA.

† Professor of Engineering Science, Department of Mechanical Engineering. Member AIAA.

The stream function is set equal to zero on one of the surfaces and equal to $B(t)$, as yet an unknown value, on the other. To derive a constraint to determine this value, first consider an instantaneous streamline OP and its normal ON. The equation of motion along the streamline can be written as

$$\partial q/\partial t + q(\partial q/\partial s) = -(1/\rho)(\partial p/\partial s) - \nu(\partial \omega/\partial n) \quad (1)$$

where q is the speed along OP and ds, dn are elements of the arcs OP and ON, respectively. On integration of the above equation around a closed streamline, one obtains

$$-\nu \oint (\partial \omega/\partial n)\, ds = \oint (\partial q/\partial t)\, ds \quad \text{or} \quad \oint (\partial \omega/\partial n)\, ds = 0 \quad (2)$$

if q is independent of time (for example, at the boundary of a stationary, impervious solid).

To develop further the consequences of this constraint, it is convenient to take the stream function as

$$\psi(\alpha, \beta, t) = \psi_1(\alpha, \beta, t) + B(t)\psi_2(\alpha, \beta) \quad (3)$$

Here, ψ_1 and ψ_2 are chosen to satisfy the Poisson's equations

$$\Delta_1 \psi_1 = -\omega_1 \quad (4)$$

and

$$\Delta_1 \psi_2 = -\omega_2;\ \omega_2 \equiv 0 \text{ except on boundaries} \quad (5)$$

where Δ_1 is the two-dimensional Laplacian operator and ω_1, ω_2 refer to vorticities corresponding to ψ_1 and ψ_2, respectively.

The boundary conditions imposed on ψ_1 and ψ_2 are depicted in Figs. 2 and 3; collectively, they must satisfy those on ψ.

For the purpose of illustration, the case of flow between two eccentric cylinders is shown when the inner cylinder is rotating with unit speed. A bipolar coordinate system is most appropriate for this geometry. Knowledge of the clearance, ($c = r_2 - r_1$), the eccentricity ratio, (ε = distance between centers/c), and the radii, r_1, r_2, of the inner and outer cylinders, respectively, is sufficient to fully determine the geometrical configuration in terms of the bipolar coordinates (α, β). Extension to the other geometries is straightforward.

The boundary constraints shown in Figs. 2 and 3 are modified appropriately if the inner cylinder is held fixed and the outer cylinder is rotating. It may appear that the Poisson equations for ψ_1 and ψ_2 are being subjected to more boundary conditions than they can tolerate. Since in the ultimate analysis, ψ satisfies a fourth-order differential equation it is mathematically justifiable to prescribe two conditions at each boundary. Only for convenience has the fourth-order equation been replaced by two second-order equations. Indeed, the algorithms developed for solution of ψ_1, ψ_2 problems are suitable only if these equations are considered as part of the fourth order system, and not for the solution of Poisson equations per se.

The function $B(t)$ is evaluated by applying the pressure periodicity condition to the stationary cylinder. Thus from Eq. (2), one obtains

$$\oint \left.\frac{\partial \omega_1}{\partial \alpha}\right|_{\alpha_2} d\beta + B(t) \oint \left.\frac{\partial \omega_2}{\partial \alpha}\right|_{\alpha_2} d\beta = 0$$

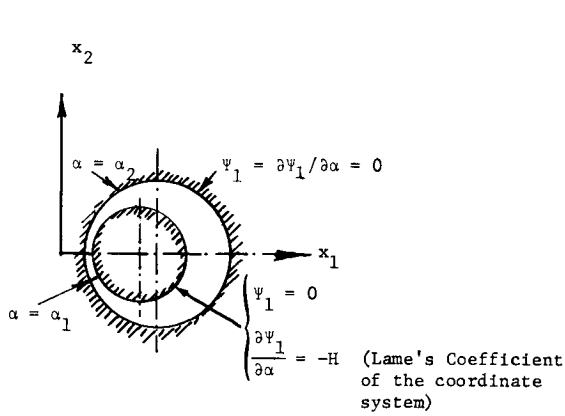

Fig. 2 ψ_1**-problem.**

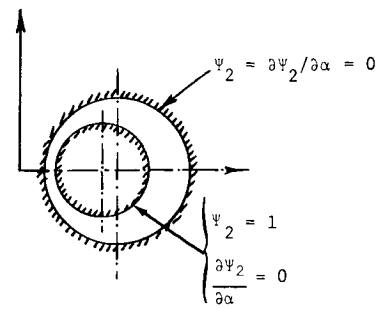

Fig. 3 ψ_2**-problem.**

or

$$B(t) = -\int_{-\pi}^{\pi} \left.\frac{\partial \omega_1}{\partial \alpha}\right|_{\alpha_2} d\beta \Big/ \int_{-\pi}^{\pi} \left.\frac{\partial \omega_2}{\partial \alpha}\right|_{\alpha_2} d\beta \quad (6)$$

The vorticity values are advanced from one time step to the next through an explicit form of the finite difference analog of the vorticity transport equation. If one is interested in only the steady-state solution, a Gauss-Siedel type of iterative procedure is preferable. In such a scheme, new values of the vorticity function are used as soon as they become available, instead of using only the old values as is the case in an explicit scheme. Considerable saving in computer time is realized through this procedure, because a time-step ten times as much as is permissible in an explicit scheme may be employed. However, experience shows that the field should be preferably swept from the stationary boundary to the moving boundary. This procedure enhances computational stability.

Solutions to the ψ_1 problem and the ψ_2 problem are obtained from finite-difference approximations to the corresponding Poisson equations. Such an equation may be written as

$$\frac{1}{H^2}\left(\frac{\partial^2 \psi}{\partial \alpha^2} + \frac{\partial^2 \psi}{\partial \beta^2}\right) = -\omega \quad (7)$$

Most of the orthogonal coordinate systems of practical interest, i.e., Cartesian, bipolar, cylindrical-polar [after transformation of the radial coordinate r to $\alpha = \ln(r)$] and parabolic-cylindrical, admit a relation of the aforementioned form. To develop a more accurate finite difference analog of the Poisson's equation, than the usual 5-point one, both sides of Eq. (7) are multiplied by an averaging kernel and subsequently integrated over the region $(-\Delta\alpha, \Delta\alpha)$ and $(-\Delta\beta, \Delta\beta)$. Thus Eq. (7) becomes

$$\int_{-1}^{1}\int_{-1}^{1} (1-|\xi|)(1-|\zeta|)\left[\frac{1}{(\Delta\alpha)^2}\frac{\partial^2 \psi}{\partial \xi^2} + \frac{1}{(\Delta\beta)^2}\frac{\partial^2 \Psi}{\partial \zeta^2}\right] d\xi\, d\zeta = \int_{-1}^{1}\int_{-1}^{1} (1-|\xi|)(1-|\zeta|)(-\omega H^2)\, d\xi\, d\zeta \quad (8)$$

where

$$\xi = \alpha/(\Delta\alpha) \quad \text{and} \quad \zeta = \beta/(\Delta\beta)$$

The requisite integrations are carried out on the assumption that a) $\partial^2\psi/\partial^2\xi$ is cubic in ζ; b) $\partial^2\psi/\partial\zeta^2$ is cubic in ξ; and c) (ωH^2) is cubic in ξ and ζ. The 9-point algorithm relating the stream function and the vorticity function at any 9 adjoining points, so realized, can be written as

$$\begin{aligned} &K_1[\psi_{i-1,j+1} + \psi_{i+1,j+1} + \psi_{i-1,j-1} + \psi_{i+1,j-1}] + \\ &K_2[\psi_{i,j+1} + \psi_{i,j-1}] + K_3[\psi_{i-1,j} + \psi_{i+1,j}] + \\ &\tfrac{10}{6}[-1 - (\Delta\alpha/\Delta\beta)^2]\psi_{i,j} = [(\Delta\alpha)^2/144][\phi_{i-1,j+1} + \\ &\phi_{i+1,j+1} + \phi_{i-1,j-1} + \phi_{i+1,j-1} + 10(\phi_{i,j+1} + \phi_{i,j-1} + \\ &\phi_{i-1,j} + \phi_{i+1,j}) + 100\phi_{i,j}] \end{aligned} \quad (9)$$

where

$$K_1 = [1 + (\Delta\alpha/\Delta\beta)^2]/12; \quad K_2 = [-1 + 5(\Delta\alpha/\Delta\beta)^2]/6$$
$$K_3 = [5 - (\Delta\alpha/\Delta\beta)^2]/6$$

$\phi_{i,j} = (-\omega H^2)_{i,j}$ and i,j = integers for the incrementation of α and β, respectively.

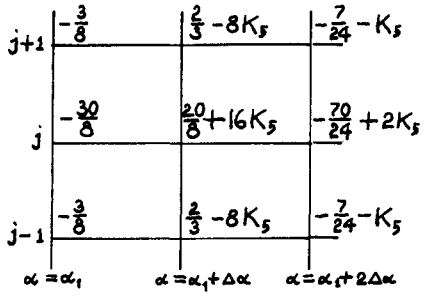

Fig. 4a Coefficients of ψ.

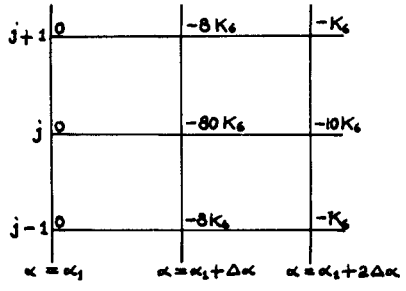

Fig. 4b Coefficients of $(-\omega H^2)$.

The system of finite-difference equations obtained from the preceding algorithm may be written as

$$[A_m][\psi_{m-1}]+[B_m][\psi_m]+[C_m][\psi_{m+1}]=[R_m] \quad (10)$$

where $[A_m]$, $[B_m]$, and $[C_m]$ are square matrices and $[\psi_m]$ is a column vector having for its elements the unknown values of ψ at $\alpha=\alpha_1+(m-1)\Delta\alpha$.

The preceding algorithm has to be modified near a boundary. Thus near $\alpha=\alpha_1$, one writes

$$\partial^2\psi/\partial\alpha^2=-\omega H^2-\partial^2\psi/\partial\beta^2 \quad (11)$$

On integration of the preceding equation twice with respect to α from $\alpha=\alpha_1$ to $\alpha_1+\Delta\alpha$, one obtains

$$\frac{1}{(\Delta\alpha)^2}[\psi(\alpha_1+\Delta\alpha,\beta)-\psi(\alpha_1,\beta)]=\frac{1}{(\Delta\alpha)}\frac{\partial\psi}{\partial\alpha}(\alpha_1,\beta)+\int_0^1(1-\xi)\chi\,d\xi \quad (12)$$

where

$$\chi=-(\omega H^2+\partial^2\psi/\partial\beta^2)$$

On the assumption that χ is quadratic in ξ, the right-hand side of Eq. (12) can be integrated. Both sides of the resulting equation are multiplied by $(1-|\zeta|)$ and integrated over the interval $[-\Delta\beta,+\Delta\beta]$ to obtain a weighted average in the β-direction as before. The equation thus obtained, however, contains the unknown values of the vorticity function, ω, at the surface $\alpha=\alpha_1$. These are eliminated by combining this equation with the interior algorithm, obtained earlier, written for $\alpha=\alpha_1+\Delta\alpha$. The final equation has the form

$$[B_2][\psi_2]+[C_2][\psi_3]=[R_2] \quad (13)$$

where $[R_2]$, the residual column vector, contains the known values of ω in the interior and the known values of ψ and $\partial\psi/\partial\alpha$ at the boundary ($\alpha=\alpha_1$). A similar procedure is adopted near the other boundary ($\alpha=\alpha_2$). The coefficients of the various terms are displayed in Figs. 4a and 4b where $K_5=(\Delta\alpha)^2/3(\Delta\beta)^2$, and $K_6=(\Delta\alpha)^2/36$, respectively.

Once the ψ-field has been computed, the vorticity at the surface is obtained from the interior algorithm written for $\alpha=\alpha_1+\Delta\alpha$ and $\alpha=\alpha_2-\Delta\alpha$. After transfer of the known quantities to the right-hand side, equation takes the form

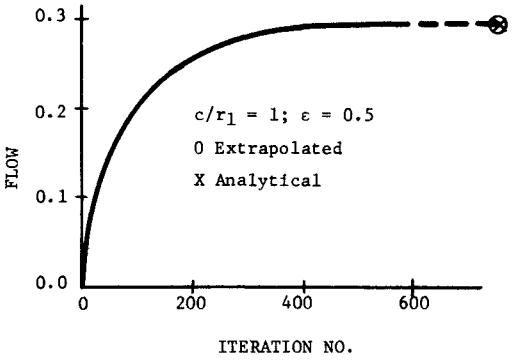

Fig. 5 Stokes flow-flow development at the rotating cylinder.

$$[B_o][\omega_s]=[R] \quad (14)$$

where $[B_o]$ is a square matrix of known coefficients and $[\omega_s]$ is a column vector having for its elements the unknown values of the vorticity at the surface. Thus the vorticity at the surface can be readily computed from

$$[\omega_s]=[B_o]^{-1}[R] \quad (15)$$

III. Summary of Computational Procedure

On the assumption that ψ^n, ω^n are known everywhere at the end of the nth iteration, the steps in the computational procedure required to go to the end of $(n+1)$th time step are: a) Obtain new values of the vorticity in the interior from the vorticity transport equation; b) Set ω_1 equal to these values and solve for ψ_1; c) Evaluate ω_1 at the surfaces; d) Compute the value of $B(t)$ from Eq. (6); and e) Obtain the values of ψ and ω from $\psi=\psi_1+B\psi_2$; and $\omega=\omega_1+B\omega_2$.

It may be noted that the vorticity is updated in two stages. First in the interior and then on the surfaces after computation of the new ψ-field.

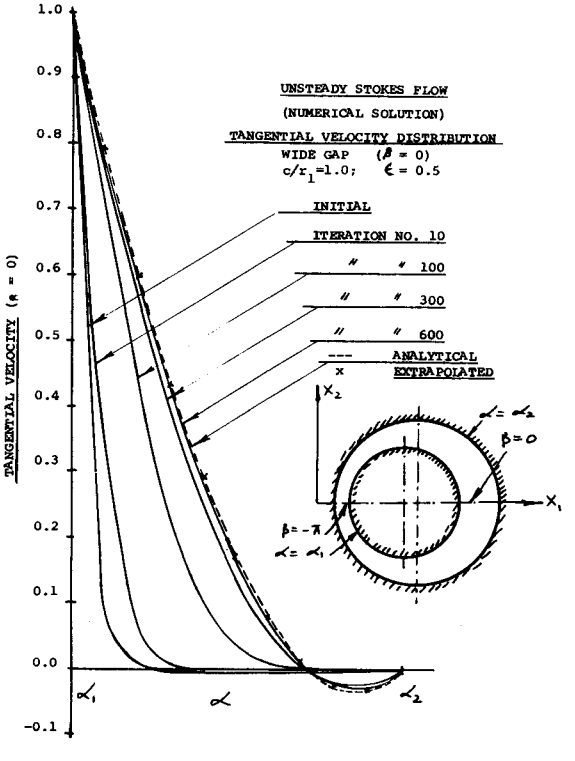

Fig. 6 Stokes flow-tangential velocity distribution in the wide gap.

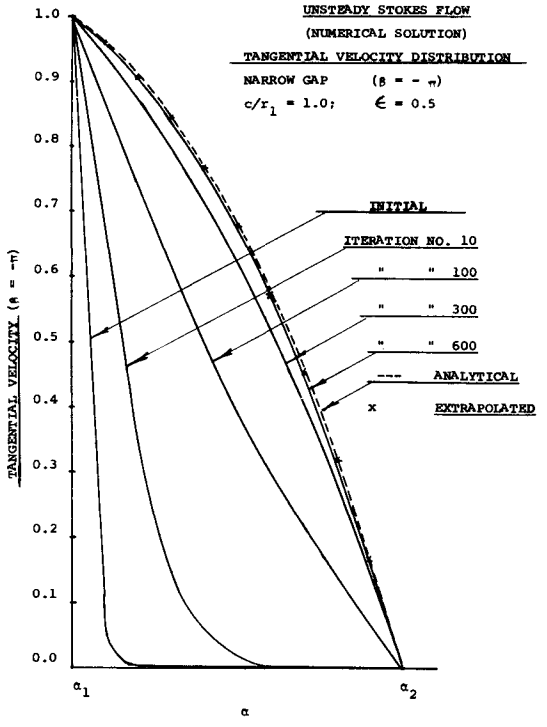

Fig. 7 Stokes flow-tangential velocity distribution in the narrow gap.

The time step is now complete. If desired, any secondary information of interest such as the pressure or the velocity can be computed.

In an approach to steady state, the iterations are terminated when

$$\frac{|\psi_{i,j}^{n+1}-\psi_{i,j}^{n}|_{\max}}{|\psi_{i,j}^{n+1}|_{\max}} \leqq 10^{-5} \tag{16}$$

The number 10^{-5} is empirical, and was chosen after some experimentation. The final steady-state values can also be obtained by exponential extrapolation from three equally spaced iterations. Thus if F_1, F_2, and F_3 are known values of some quantity at times t_1, t_2, and t_3, respectively, such that $(t_3-t_2)=(t_2-t_1)$, its asymptotic value F_∞ is given by

$$F_\infty = (F_1F_3-F_2^2)/(F_1+F_3-2F_2) \tag{17}$$

Equation (17) is obtained on the assumption that, in a linear system

$$F = F_\infty + Ae^{-\gamma t}; \quad t \to \infty$$

where F_∞, A, and γ are constants, and 't' is either the time in a bonafide transient solution, or the iteration parameter in a "forced" solution.

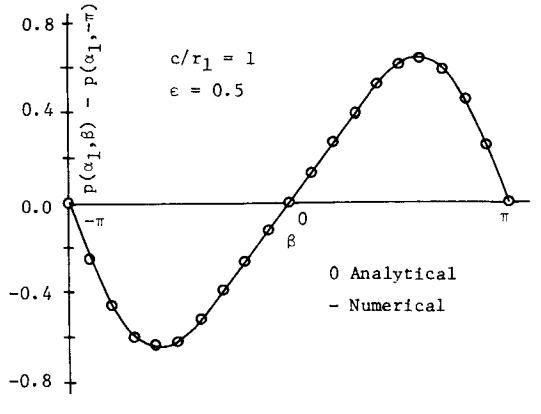

Fig. 8 Stokes flow-pressure distribution on the inner cylinder.

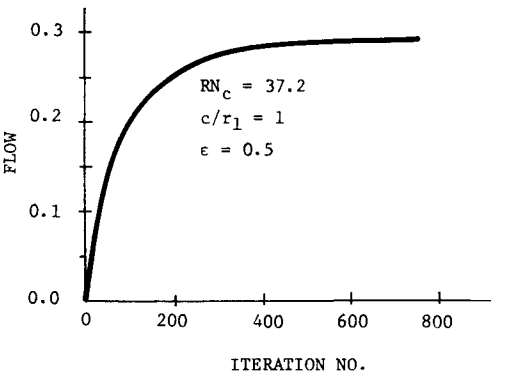

Fig. 9 Navier-Stokes flow-flow development at the rotating cylinder.

Equation (17) has been used to predict the final steady-state values for the Stokes flow. The close agreement between the extrapolated and the analytical values, as is evident from Figs. 5–7, testifies to the validity of Eq. (17).

IV. Results and Discussion

a. Numerical Results from the Stokes Flow

An analytical solution of the Stokes flow between two, long, eccentric cylinders when either of them is rotating is available in the literature and has been reported by various authors including Kamal.[2]‡ Therefore, it was deemed advisable to apply the computational procedure to this flow to obtain a check on the validity and accuracy of the proposed method. Numerical results were obtained for a clearance ratio of 1§ and an eccentricity ratio of 0.5, with 11 stations across the gap and 21 stations around the gap. The outer cylinder is stationary, while the inner cylinder is given, impulsively, a speed of unity at $t = 0$. Figures 5–8 show some of the results obtained. In Fig. 5, the nondimensional flow Q (stream function) is shown as it develops with time at the rotating cylinder. The asymptotic trend towards a steady-state value is clearly discernible. Equation (17) can be used to extrapolate to the steady-state value of Q from its known values at iteration numbers 500, 550, and 600. This gives $Q = 0.2951781$ as compared with $Q = 0.2951452$ obtained from the analytical solution. Figure 6 shows development of the tangential velocity profiles across the widest part of the gap ($\beta = 0$). The velocities near the stationary cylinder eventually become negative. A region

Table 1 Comparison of computed and analytical values of the vorticity function at the two cylinders[a]

		Inner cylinder		Outer cylinder	
$\pm\beta/\pi$	$\pm\theta$	Computed	Analytical	Computed	Analytical
1.0	3.141	0.180	0.183	−3.061	−3.062
0.9	2.926	0.069	0.069	−2.909	−2.909
0.8	2.704	−0.243	−0.241	−2.486	−2.486
0.7	2.471	−0.662	−0.662	−1.889	−1.888
0.6	2.220	−1.088	−1.087	−1.241	−1.241
0.5	1.943	−1.419	−1.421	−0.662	−0.662
0.4	1.632	−1.609	−1.609	−0.227	−0.227
0.3	1.282	−1.655	−1.655	0.039	0.041
0.2	0.888	−1.606	−1.607	0.171	0.169
0.1	0.456	−1.537	−1.537	0.212	0.212
0.0	0.000	−1.506	−1.506	0.220	0.220

[a] $c/r_1 = 1.0$; $\varepsilon = 0.5$; θ in radians, measured from the center of the inner cylinder.

‡ There is a misprint in Kamal's paper; the third line of Eq. (26) should read $+CH\delta(\delta^2-SH^2\delta)$.

§ This particular value was chosen to permit detailed comparison with Kamal's work.

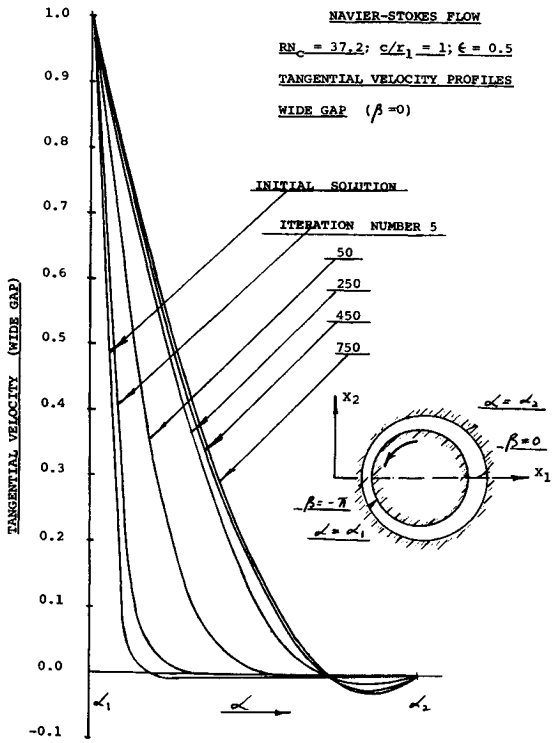

Fig. 10 Navier-Stokes flow-tangential velocity distribution in the wide gap.

of "reversed flow" exists there caused by the development of negative pressure in the lower half of the geometry. The close agreement between the analytical values and the extrapolated values should be noted. Figure 7 shows similar profiles for the narrowest portion of the gap ($\beta = \pm\pi$). Figure 8 shows the pressure distribution on the inner cylinder. In Table 1, numerical

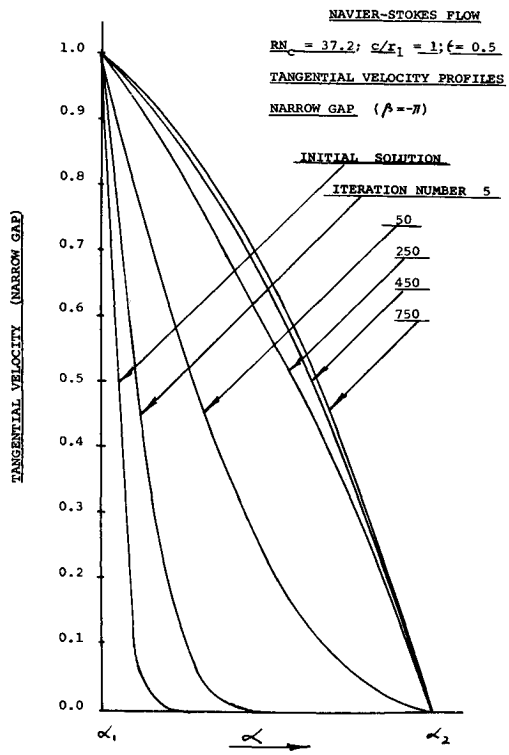

Fig. 11 Navier-Stokes flow-tangential velocity distribution in the narrow gap.

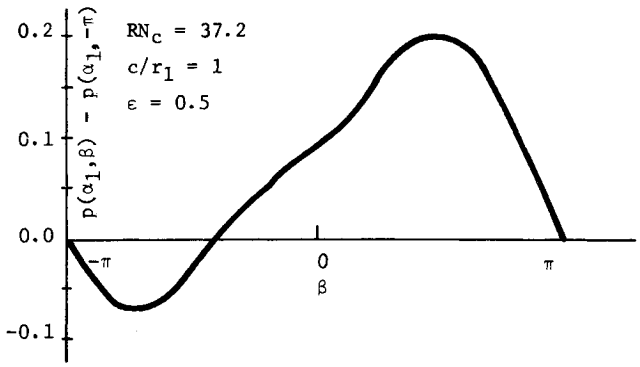

Fig. 12 Navier-Stokes flow-pressure distribution on the inner cylinder.

values of the vorticity function, both computed and analytical, are given.

b. Results from the Navier-Stokes Flows

Figures 9–12 show some of the results obtained for the full Navier-Stokes equations. The outer cylinder is stationary while the inner cylinder rotates with unit speed. The Reynolds number RN_c is 37.2 Geometrical parameters, i.e., clearance ratio and eccentricity ratio are the same as those for the Stokes flow. Again the domain of interest is spanned by an (α, β) mesh with 11 stations across the gap and 21 stations around the gap. Qualitatively, the curves are very much like those for the Stokes flow presented earlier. This is not surprising, because at such a low Reynolds number the viscous effects are likely to predominate over the inertia effects. However, some asymmetry in the pressure distribution (see Fig. 12) is observed.

In the previous computation, the pressure was set arbitrarily equal to zero on the inner cylinder at the point of narrowest gap. The momentum equations are then used to compute the pressure at an arbitrary mesh point. Thus, starting from $\beta = -\pi$, if one goes around a circle (α = const) one must end up with the value at the starting point. Earlier investigators, notably Thoman and Szewczyk,[4] found considerable "mismatch" which they attributed to "errors inherent in numerical differentiation." In the present investigation, "mismatch" is almost negligible. In Fig. 13, separation streamlines are shown for both the Stokes flow and the Navier-Stokes flow.

The flow parameters used above (that is, the Reynolds number, the clearance ratio and the eccentricity ratio) were selected so that a comparison could be made with the results of Kamal.[2] However, the absence of numerical data in Ref. 2 makes accurate comparison difficult. The separation streamline of the Stokes flow

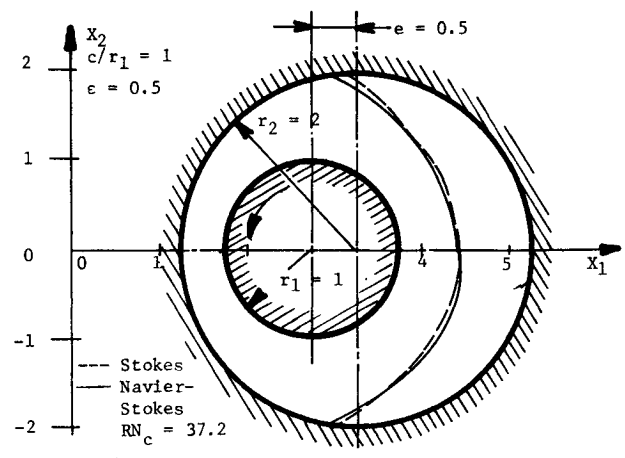

Fig. 13 Separation streamlines.

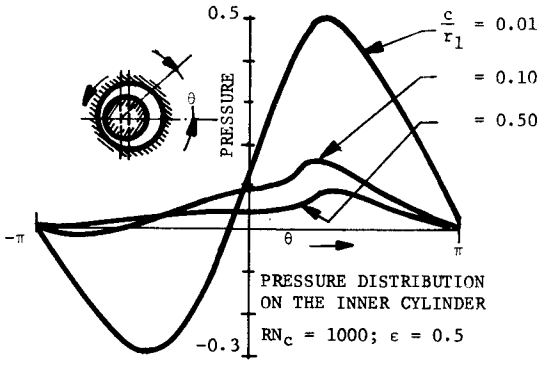

Fig. 14 Effect of clearance ratio on pressure distribution.

drawn in Figs. 4 and 5 of Ref. 2 seems to give an erroneous location of the point of stagnation on the outer cylinder.

It is well known that, if the inner cylinder is rotating, two-dimensional flows persist only when the Taylor number ($Tn = RN_c^*(c/r_1)^{1/2}$) is below 41.6. For greater Taylor numbers, vortices appear in the annulus, making the flow three dimensional. Eventually, at high Reynolds numbers, the flow becomes turbulent. However, if the outer cylinder is rotating, and the inner cylinder is stationary, two-dimensional laminar flow may persist up to a Reynolds number of 1500 (Ref. 5). Therefore, to examine the effect of inertia further, the case of an outer cylinder rotating with the inner cylinder stationary was next considered.

Figure 14 shows the effects of changing the clearance ratio upon the pressure distribution around the inner cylinder. Here the eccentricity ratio is 0.5 and the Reynolds number is 1000. As the clearance ratio is increased, a marked asymmetry in the pressure distribution develops, indicating the increased influence of inertia. The peak pressure occurs near the widest gap and is not affected much by changing the clearance ratio. If inertia is neglected, the pressure would be antisymmetrical about $\theta = 0$. Calculations of Yamada and Nakabyashi[5] yielded the same pressure at $\theta = 0$, irrespective of clearance. This result contradicts our own findings, as can be seen from the curves in Fig. 14.

In Fig. 15, the effect of the Reynolds number on the pressure distribution around the inner cylinder is shown. Here the clearance ratio is 1 and the eccentricity ratio is 0.5. In comparing the various pressure curves, one should recall that the pressure is normalized by the factor (ρV^2) which differs materially from one curve to the next. Again, the marked asymmetry in the pressure distributions reflects the increased influence of inertia.

In Fig. 16, the effect of changing eccentricity ratio is exhibited. As the eccentricity is increased (at a fixed clearance ratio and a fixed Reynolds number), the pressure distribution shows a rapid change in the converging section of the geometry. This is the well known effect utilized for lubrication.

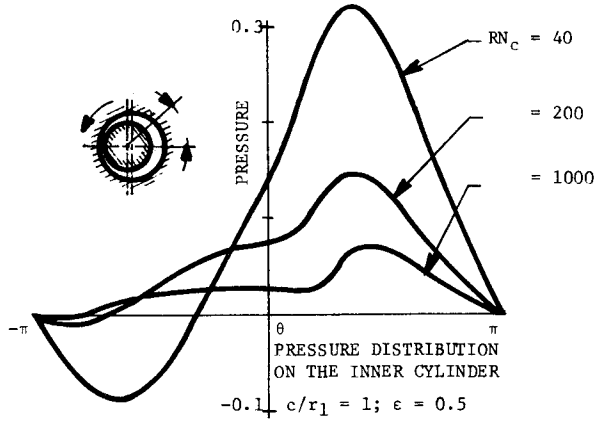

Fig. 15 Effect of Reynolds number on pressure distribution.

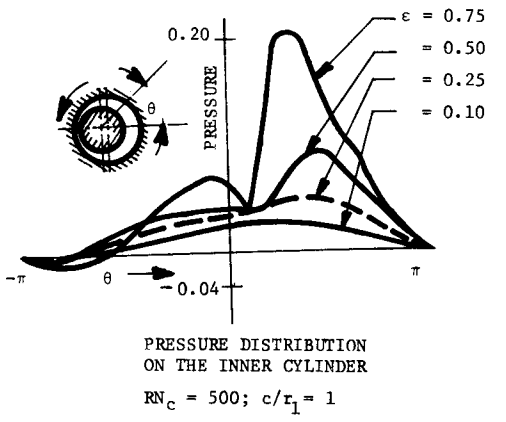

Fig. 16 Effect of eccentricity on pressure distribution.

V. Conclusions

A technique has been presented for the numerical solution of the incompressible viscous flow equations of a Newtonian fluid. The fluid is assumed to have constant properties, and solution is effected by using coupled differential equations; namely, Poisson's equation for the stream function and the convective diffusion equation for the vorticity. The numerical algorithms employed can sustain extremely high gradients normal to boundaries of the flow. These algorithms can be generalized to any orthogonal, curvilinear system of coordinates. All boundary conditions on the stream function are handled in clear-cut fashion. In particular, single-valuedness of the pressure is directly imposed for doubly-connected regions.

To test the numerical procedures on a relatively simple geometry, a study was made of the two-dimensional laminar flow in the annulus between two cylinders, one of which is rotating. Transient and steady-state results were obtained for both Stokes equation (inertia neglected) and the full Navier-Stokes equation. Rotational speeds of the inner cylinder were explored up to the point of incidence of Taylor vortices, and the outer cylinder speed effects were investigated for the entire extent of laminar flow.

In the case of Stokes flow, exact analytical results are available. Our numerical results for the stream function and for the pressure agree with those from the analysis to better than two significant figures when the chanel is divided into ten "radial" segments and 20 angular segments. For the geometry in question, it is anticipated that the inclusion of inertia terms does not appreciably affect the solution accuracy. Of course, no exact analytical results are available for comparison. Computation times for typical cases were less than 5 min on the IBM-360-75/91.

References

[1] Fromm, J. E., "A Method for Computing, Nonsteady, Incompressible, Viscous Fluid Flows," Rept. L.A. 2910, 1963, Los Alamos Scientific Lab., Los Alamos, N. Mex.

[2] Kamal, M. M., "Separation in the Flow Between Eccentric Rotating Cylinders," *Journal of Basic Engineering*, Vol. 88, Ser. D, No. 4, Dec. 1966, p. 717.

[3] Runchal, A. K., Spalding, D. B., and Wolfshtein, M., "Numerical Solution of the Elliptic Equations for Transport of Vorticity, Heat and Matter in Two-Dimensional Flow," *Physics of Fluids*, Suppl. II, Dec. 1969, pp. 11–21.

[4] Thoman, D. C. and Szewczyk, A. A., "Time-Dependent Viscous Flow Over a Circular Cylinder," *Physics of Fluids*, Suppl. II, Dec. 1969, pp. 11–76.

[5] Yamada, Y. and Nakabayashi, K., "On the Flow Between Eccentric Cylinders When the Outer Cylinder Rotates," *Bulletin, Japan Society of Mechanical Engineers*, Vol. 11, No. 45, 1968, p. 455.

[6] Sood, D. R., "On the Numerical Solution of the Navier-Stokes Equations in a Doubly-Connected Region," Ph.D. thesis, 1971, Dept. of Mechanical Engineering, Columbia Univ., New York.